Synthesis, characterisation and bioimaging of a fluorescent rhenium-containing PNA bioconjugate

Gasser, Gilles ; Pinto, Antonio ; Neumann, Sebastian ; Sosniak, Anna M ; Seitz, Michael ; Merz, Klaus ; Heumann, Rolf ; Metzler-Nolte, Nils

Abstract: A new rhenium tricarbonyl complex of a bis(quinoline)-derived ligand (2-azido-N,N-bis((quinolin-2-yl)methyl)ethanamine, L-N(3)), namely [Re(CO)(3)(L-N(3))]Br was synthesized and characterized in-depth, including by X-ray crystallography. [Re(CO)(3)(L-N(3))]Br exhibits a strong UV absorbance in the range 300-400 nm with a maximum at 322 nm, and upon photoexcitation, shows two distinct emission bands at about 430 and 560 nm in various solvents (water, ethylene glycol). [Re(CO)(3)(L-N(3))]Br could be conjugated, on a solid phase, to a peptide nucleic acid (PNA) oligomer using the copper(I)-catalyzed azide-alkyne cycloaddition reaction (Cu-AAC, "click" chemistry) and an alkyne-containing PNA building block to give Re-PNA. It was demonstrated that upon hybridisation with a complementary DNA strand (DNA), the position of the maxima and emission intensity for the hybrid Re-PNA · DNA remained mainly unchanged compared to those of the single strand Re-PNA. The rhenium-containing PNA oligomer Re-PNA could be then mediated in living cells where they have been shown to be non-toxic contrary to the general notion that organometallic compounds are usually unstable under physiological conditions and/or cytotoxic. Furthermore, Re-PNA could be detected in living cells using fluorescent microscopy.

DOI: https://doi.org/10.1039/c2dt12114j

Synthesis, Characterisation and Bioimaging of a Fluorescent Rhenium-Containing PNA Bioconjugate

Gilles Gasser,[a,b,†,*] *Antonio Pinto,*[b,†] *Sebastian Neumann,*[c,†] *Anna M. Sosniak,*[b] *Michael Seitz,*[b] *Klaus Merz,*[b] *Rolf Heumann,*[c] *and Nils Metzler-Nolte*[b,*]

[a] Institute of Inorganic Chemistry, University of Zurich, Winterthurerstrasse 190, CH-8057 Zurich, Switzerland; [b] Department of Inorganic Chemistry I – Bioinorganic Chemistry, Faculty of Chemistry and Biochemistry, Ruhr-University Bochum, Universitätsstrasse 150; 44801 Bochum, Germany; [c] Department of Biochemistry II – Molecular Neurobiochemistry, Faculty of Chemistry and Biochemistry, Ruhr-University Bochum, Universitätsstrasse 150; 44801 Bochum, Germany.

RECEIVED DATE (to be automatically inserted after your manuscript is accepted if required according to the journal that you are submitting your paper to)

[†] These authors have contributed equally to the work.

* Corresponding authors: email: gilles.gasser@aci.uzh.ch; Phone: +41 44 635 46 11. Fax: +41 44 635 68 03; WWW: www.gassergroup.com. Email: nils.metzler-nolte@rub.de; Phone: +49 234 322 8152; Fax: +49 234 321 4378 ; WWW : www.rub.de/ac1.

Keywords: Bioorganometallics, Peptide Nucleic Acid, Click Chemistry, Rhenium Compounds, Fluorescence Microscopy.

Abbreviations: Boc - *tert*-butoxycarbonyl; Bhoc -benzhydryloxycarbonyl; DIPEA – diisopropylethylamine; eGFP – enhanced Green Fluorescent Protein; ESI-MS - electrospray ionisation mass spectrometry; Fmoc – fluorenylmethoxycarbonyl; Gly - glycine; IL – intraligand; Lys – lysine; Maldi-tof – Matrix assisted laser/desorption ionization - time of flight; MLCT - Metal to Ligand Charge Transfer; PNA – peptide nucleic acid; SPPS – solid phase peptide synthesis; TFA – trifluoroacetic acid; TIS - triisopropylsilane.

Abstract.

A new rhenium tricarbonyl complex of a bis(quinoline)-derived ligand (2-azido-*N,N*-bis((quinolin-2-yl)methyl)ethanamine, **L-N_3**), namely **[$Re(CO)_3$(L-N_3)]Br** was synthesized and characterized in-depth, including by X-ray crystallography. **[$Re(CO)_3$(L-N_3)]Br** exhibits a strong UV absorbance in the range 300-400 nm with a maximum at 322 nm, and upon photoexcitation, shows two distinct emission bands at about 430 and 560 nm in various solvents (water, ethylene glycol). **[$Re(CO)_3$(L-N_3)]Br** could be conjugated, on the solid phase, to a peptide nucleic acid (PNA) oligomer using the copper(I)-catalyzed azide-alkyne cycloaddition reaction (Cu-AAC, "click" chemistry) and an alkyne-containing PNA building block to give **Re-PNA**. It was demonstrated that upon hybridisation with a complementary DNA strand (**DNA**), the position of the maxima and emission intensity for the hybrid **Re-PNA•DNA** remained mainly unchanged compared to those of the single strand **Re-PNA**. The rhenium-containing PNA oligomer **Re-PNA** could be then mediated in living cells where they have been shown to be non-toxic contrary to the general notion that organometallic compounds are usually unstable under physiological conditions and/or cytotoxic. Furthermore, **Re-PNA** could be detected in living cells using fluorescent microscopy.

Introduction

Peptide Nucleic Acids (PNAs) are non-natural nucleic acid analogues.[1, 2] The usual phosphate-ribose backbone of DNA/RNA is replaced in PNA by a neutral pseudo-peptide backbone made of *N*-(2-aminoethyl)glycine units, which are ligated, via a methylene carbonyl group, to one of the four nucleobases.[1] PNAs possess attractive properties, which include good chemical stability, resistance to nucleases and proteases, high binding affinity for DNA/RNA strands, great discrimination of single-base mismatches, and fast hybridization kinetics. These favorable characteristics have led to the investigation of PNAs, for example, as agents in antisense[3-5] and antigene therapy.[6-8]

The covalent attachment of metal complexes to PNA oligomers is currently being intensively investigated all around the world.[9] These metal conjugates have found applications in various research fields such as radioactive probes, as in the sequence-specific detection of nucleic acids, in the hydrolysis of nucleic acids and peptides, or as modulators of PNA•DNA hybrid stability.[9] However, to the best of our knowledge, there has been no report, to date, of the utilization of metal-PNAs for gene silencing. This is rather surprising as the addition of a specific metal complex to a PNA oligomer can be of significant interest. Our group[10] and Krämer *et al.*[11] have, for example, demonstrated that simply attaching a metal complex to PNA bioconjugates can significantly increase the cellular uptake of PNA. Recently, Licandro and co-workers have reported the preparation and photophysical properties of luminescent dinuclear rhenium(I) tricarbonyl complex-PNA conjugates.[12] One of their Re-PNA conjugates showed interesting two-photon absorption properties, which was exploited for imaging experiments in HEK-293 cells.[12]

In the present study, a fluorescent metal complex was covalently linked to a PNA oligomer. We were curious to investigate to which extend the presence of a metal complex would affect the intrinsic biological properties of the resulting bioconjugate. As a note of caution, Barton *et al.* have studied the mechanism of cellular uptake of a series of ruthenium complexes and Ru-peptide bioconjugates.[13-17] They demonstrated how the addition of an organic fluorophore to inorganic fluorophore-tagged cell-

penetrating peptide (CPP) bioconjugates induced a change in transport pathway as well as in subcellular distribution of the new bioconjugate.[15] These discoveries further emphasize the interest of employing metallo-fluorophores. Indeed, contrary to a "normal" organic fluorophore, the presence of a metal complex not only allows lifetime imaging but can also lead to further opportunities such as the use of Atomic Absorption Spectroscopy (AAS) to quantify the uptake of the conjugates.[5]

Herein, we present the preparation and in-depth characterization, including X-ray crystallography, of a novel rhenium tricarbonyl complex (**[Re(CO)$_3$(L-N$_3$)]Br**, Figure 1) of a bis-quinoline derivative ligand, 2-azido-*N*,*N*-bis((quinolin-2-yl)methyl)ethanamine (**L-N3**, Figure 1), which was selected in this work as the organometallic moiety of choice. Re tricarbonyl complexes with similar ligands have been indeed shown to have favorable optical properties such as large Stokes shift, long lifetime, and polarized emission. Due to their good chemical stability and facile preparation, these complexes as well as their ^{99m}Tc congeners, were already used for the (radio-)labeling of biomolecules by Zubieta, Valliant, Babich and our groups for both *in vitro* and *in vivo* imaging purposes.[18-30] We then report on the facile coupling of **[Re(CO)$_3$(L-N$_3$)]Br**, on the solid-phase, to an alkyne-containing PNA oligomer (**Re-PNA**). The possibility to detect **Re-PNA** in living cells by fluorescence microscopy is also presented. A high binding affinity of this metal-PNA bioconjugate to complementary DNA was confirmed by UV melting studies.

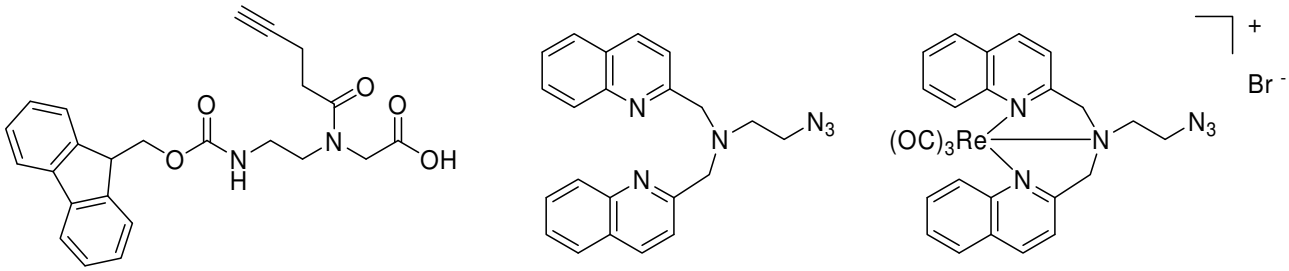

Fmoc-1-OH **L-N$_3$** **[Re(CO)$_3$(L-N$_3$)]Br**

Figure 1. Structures of **Fmoc-1-OH**, **L-N3** and **[Re(CO)$_3$(L-N$_3$)]Br.**

Results and discussion

Synthesis and characterization of [Re(CO)$_3$(L-N$_3$)]Br. 2-Azido-*N*,*N*-bis((quinolin-2-yl)methyl)ethanamine (**L-N$_3$**) was obtained by reacting 2-(bis((quinolin-2-yl)methyl)amino)ethanol (**L-OH**)[31] with triphenyl phosphine, diisopropyl azodicarboxylate and diphenylphosphoryl azide in THF following a similar procedure described by our groups (Scheme 1).[32] The presence of **L-N$_3$** was ascertained by IR spectroscopy with a strong vibration at 2093 cm^{-1} corresponding to the azide function. The Re complex **[Re(CO)$_3$(L-N$_3$)]Br** could then be obtained in good yield by refluxing **[NEt$_4$][ReBr$_3$(CO)$_3$]**[33] with **L-N$_3$** in methanol. As expected, **[Re(CO)$_3$(L-N$_3$)]Br** exhibits a sharp, strong band at 2025 cm^{-1} and a broad and intense absorption at 1897 cm^{-1}, attributed to the ν(C-O) bands of A and E symmetry of the *fac*-[Re(CO)$_3$] moiety, as well as another strong band at 2101 cm^{-1} corresponding to the azide function. In ESI-MS, the base peak at *m/z* = 639 was assigned to **[Re(CO)$_3$(L-N$_3$)]$^+$**, with the expected isotope fingerprint of ^{185,187}Re observed. The ^{1}H-NMR spectrum of **[Re(CO)$_3$(L-N$_3$)]Br** in CD$_3$OD showed two sets of doublets at about 5.30 ppm, corresponding to the four methylene protons adjacent to the quinoline rings (Figure S2 in the SI).[19] In comparison, for **L-N$_3$**, only a singlet is observed for these four protons (Figure S1 in the SI). In CD$_3$OD, the four methylene protons adjacent to the quinoline rings are rapidly exchanged with deuterium as shown by mass spectrometry and NMR spectroscopy (Figures S3–5 in the SI), paralleling similar behavior in other Re tricarbonyl complexes that we have recently reported.[32]

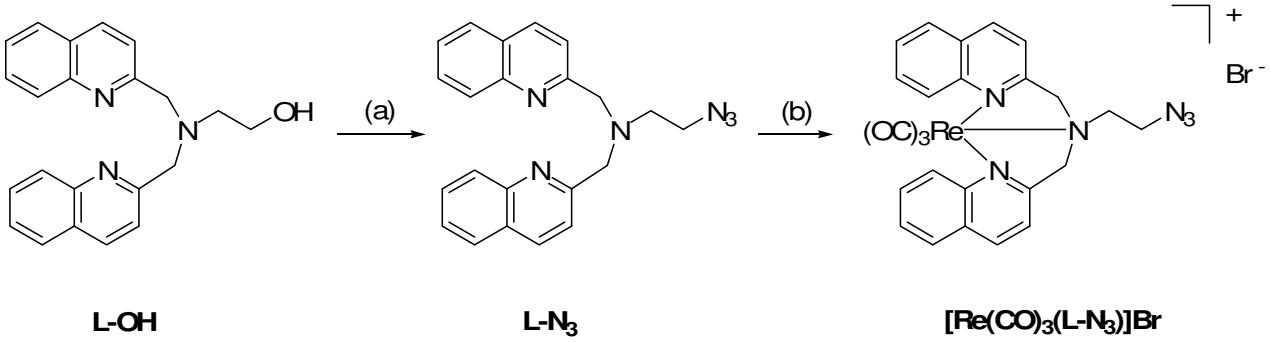

L-OH **L-N$_3$** **[Re(CO)$_3$(L-N$_3$)]Br**

Scheme 1. Synthesis of **[Re(CO)$_3$(L-N$_3$)]Br**. (a) PPh$_3$, diisopropyl azodicarboxylate, diphenylphosphoryl azide, THF, 72h, 32% (b) **[NEt$_4$]$_2$[Re Br$_3$(CO)$_3$]**, MeOH, 3h, 84%.

X-ray crystallography of [Re(CO)$_3$(L-N$_3$)]Br. Figure 2 shows the molecular structure of the Re tricarbonyl complex **[Re(CO)$_3$(L-N$_3$)]Br**. The coordination number around each Re centre is six in an approximate octahedral coordination environment. The Re-C bond distances (1.904(10) to 1.940(10) Å) and the nearly linear azido group (N4-N5 1.220(14), N5-N6 1.110(16), N4-N5-N6 173.1(14)) in **[Re(CO)$_3$(L-N$_3$)]Br** are reminiscent of related Re complexes[34, 35] and azido compounds.[36, 37]

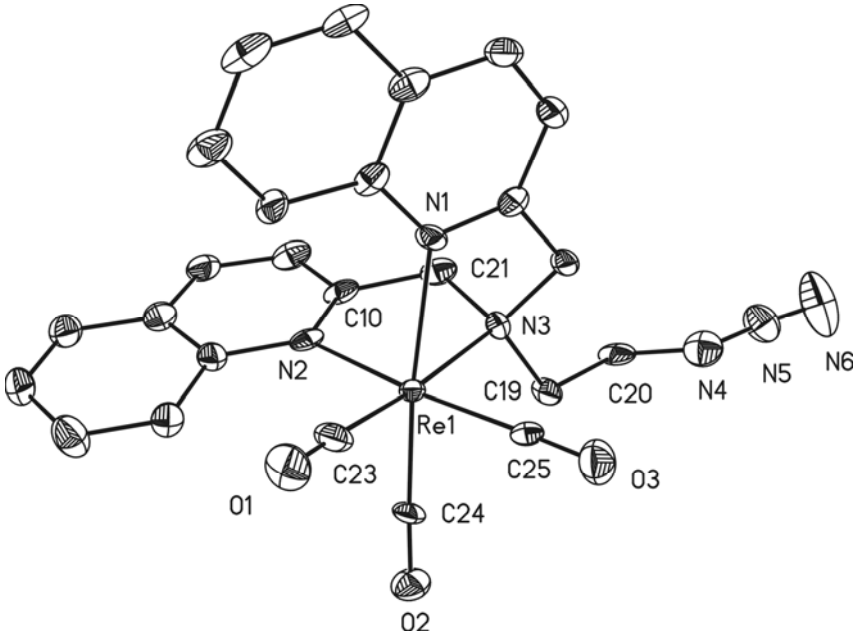

Figure 2. ORTEP plot of **[Re(CO)$_3$(L-N$_3$)]Br** in the asymmetric unit at 50 % probability levels. Selected bond distances (Å) and angles (°): Re1-C23 1.936(11), Re1-C24 1.904(10), Re1-C25 1.940(10), C23-O1 1.127(14), C24-O2 1.143(13), C25-O3 1.126(13), N3-C19 1.478(13), C19-C20 1.545(14), C20-N4 1.466(16), N4-N5 1.220(14), N5-N6 1.110(16), N3-C19-C20 116.4(8), C19-C20-N4 108.9(9), C20-N4-N5 114.7(10), N4-N5-N6 173.1(14).

Optical properties of [Re(CO)$_3$(L-N$_3$)]Br. The photophysical data of **[Re(CO)$_3$(L-N$_3$)]Br** are comparable to those previously reported by Zubieta *et al.* for related bis-quinoline Re tricarbonyl complexes.[18, 19, 22] **[Re(CO)$_3$(L-N$_3$)]Br** exhibits a strong UV absorbance in the range 300-400 nm with a maximum at 322 nm (see Figure S6 in the SI). These transitions most likely have considerable metal-to-ligand-charge-transfer (MLCT: d_π(Re) –> π^*(ligand)).[19]

Upon photoexcitation, the rhenium complex shows two distinct emission bands at about 430 and 560 nm in various solvents (e.g. water, ethylene glycol). Ethylene glycol was found to enhance the intensity of the band at 560 nm (relative to the one at 430 nm, see Figure 4). The high-energy transition is assigned to ligand-centered fluorescence, whilst the lower energy transition originates from a ^{3}MLCT state (see Figure 3 for emission spectra of **[Re(CO)$_3$(L-N$_3$)]Br** and Table 1 for a summary of its photophysical data). Luminescence lifetime measurements for the emission at 560 nm (λ_{exc} = 325 nm) were carried out in both degassed and air-saturated ethylene glycol, giving single exponential decays in both cases (Figure S7 in the SI). The lifetime in the presence of dioxygen is considerably shorter (τ = 3.97 ± 0.57 μs) compared to degassed solutions (τ = 10.65 ± 0.14 μs), which is a common phenomenon and characteristic for ^{3}MLCT emissions.[18, 38] Also in accordance with our tentative assignment of a charge-transfer transition is the observation of a strong solvent-dependence of the quantum yields for this band (Table 1).

Table 1. Photophysical data for complex **[Re(CO)$_3$(L-N$_3$)]Br** at room temperature.

Medium	Excitation λ_{exc} / nm	Emission λ_{em} / nm	Quantum Yields Φ / % [a]
Degassed Ethylene glycol	317	430, 560	0.14, 0.48
Degassed Ethylene glycol	325	430, 560	0.12, 0.50
Degassed Ethylene glycol	347	430, 560	0.26, 0.51
Air-saturated Water	317	430, 560	0.19, 0.14
Air-saturated Water	325	430, 560	0.19, 0.14

[a] Determined relative to quinine sulfate (Φ = 54.6%) in 0.5 M sulfuric acid as standard. Estimated errors are ± 30%.

Interestingly, the excitation wavelength in degassed ethylene glycol had an effect on the quantum yields Φ of the band at 430 nm (Φ ranging from 0.12 % to 0.26 %) but not for the "metal-transition" at 560 nm where Φ remains stable at about 0.50 %. The absolute values for the quantum yields are only slightly lower than others previously reported for similar Re compounds.[18, 20, 38, 39]

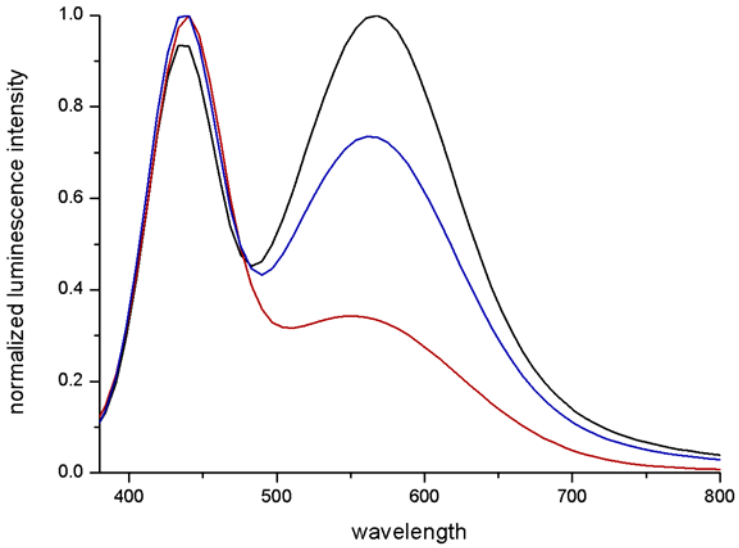

Figure 3. Normalized emission spectra of $[Re(CO)_3(L\text{-}N_3)]Br$ in degassed ethylene glycol (black), air-saturated ethylene glycol (blue), and in air-saturated water (red) at room temperature (λ_{exc} = 325 nm).

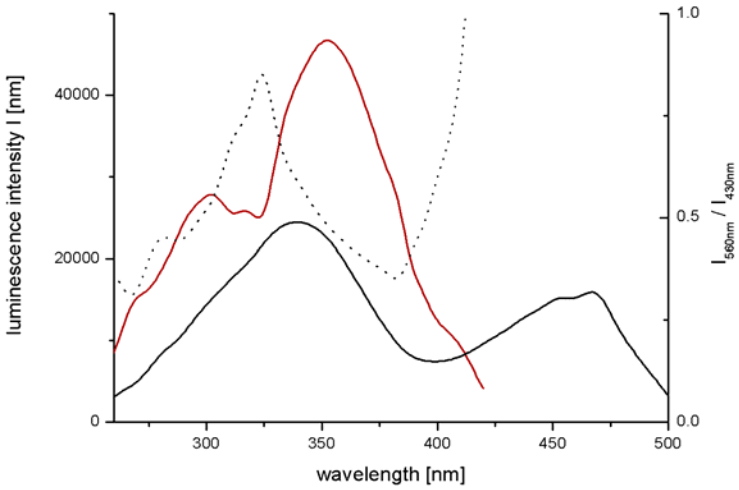

Figure 4. Excitation spectra for **[Re(CO)$_3$(L-N$_3$)]Br** in degassed ethylene glycol with emission monitored at 430 nm (red) and 560 nm (black). Ratio of luminescence intensities at 560 nm and 430 nm (dotted).

Taken together, the results of the photophysical measurements, notably the large Stokes shift and the long emission lifetimes, make our Re complexes good candidates for fluorescent probes in biological experiments (*vide infra*).

Synthesis and characterization of metal-PNA oligomers. Three different PNA oligomers were prepared in this study in order to compare their fluorescence properties as well as the role played by the Re complex in the duplex formation (Table 2). In the view of future experiments, all of them are complementary to the mRNA expressing the enhanced Green Fluorescent Protein (eGFP) in stably transfected eGFP expressing HeLa cells (HeLa-eGFP). Three types of PNA sequences were prepared for comparative purposes: a typical "naked" 20-mer PNA sequence complementary to the mRNA (abbreviated **Naked-PNA**) as well as Re-containing and rhodamine-containing PNA sequences, which are fully complementary to the mRNA expressing the eGFP (abbreviated **Re-PNA** and **Rho-PNA**). The rhodamine derivative 5/6-carboxytetramethylrhodamine (present as two regioisomers), has been selected on the grounds of its commercial availability and ability to be easily conjugated to PNA oligomers.

Table 2. Summary of the PNA oligomers used in this study.

Abbreviation	Sequence	$[M + H]^+$/ $[M]^+$ [a]	$[M + H]^+$ or $[M]^+$ [b]
Naked-PNA	H-Gly-atgaacttcagggtcagcttgc-Lys-NH_2	6180.9	6181.0
Rho-PNA	H-Rho-Gly-atgaacttcagggtcagcttgc-Lys-NH_2	6593.3	6594.7
Re-PNA	H-Gly-Re-atgaacttcagggtcagcttgc-Lys-NH_2	6998.7	[c]

[a] Calculated; [b] Experimentally determined by MALDI-TOF (see experimental); [c] Characterized by ESI-MS (see Table S1 in the ESI).

All PNA oligomers were synthesized by hand on TentaGel R Fmoc-Lys(Boc)-RAM resin using Fmoc/Bhoc-protected PNA monomers and standard protocols, as previously reported by our groups.[40] The *C*-terminal lysine residue was introduced to enhance solubility.[41] A glycine was also inserted at the *N*-terminus of the PNA sequences **Naked-PNA** and **Re-PNA** in order to avoid any *N*-acyl transfer reactions.[42] For the rhodamine-containing PNA oligomer, the fluorescent label was coupled to the PNA sequences following Corey's method, which involves a "pre-loading" of the resin with the inexpensive and unactivated sulforhodamine (see experimental section for further information).[43] **Naked-PNA** and **Rho-PNA** were unambiguously characterized by MALDI-TOF mass spectrometry and their purity confirmed by analytical HPLC (see Figures S8-10 in the SI for examples of MALDI-TOF spectra and analytical HPLC chromatograms). Various synthetic pathways were previously reported for the preparation of metal-containing PNAs.[9] In this work, we capitalize on our recent discoveries to efficiently attach organometallic complexes to peptides and PNA oligomers using the copper(I)-catalysed Huisgen 1,3-dipolar cycloaddition reaction, often referred to as "Click Chemistry".[29, 40, 44-48] In order to label the PNA oligomer with **$[Re(CO)_3(L\text{-}N_3)]Br$**, an alkyne-containing PNA monomer[44, 46, 48, 49] (**Fmoc-1-OH**, Figure 1) was inserted into a PNA sequence before the *N*-terminal glycine. The

azido-containing rhenium tricarbonyl complex **[Re(CO)$_3$(L-N$_3$)]Br** was then "clicked" to the PNA oligomer on the solid phase (see Scheme 2). After cleavage of the oligomers from the resin and successive HPLC purification, the Re-containing PNA oligomers, namely **Re-PNA**, was obtained. Its purity was confirmed by analytical HPLC and its identity was ascertained by ESI-MS as well as by IR spectroscopy, notably showing the presence of two CO bands in the 1900-2040 cm^{-1} region (see Table S1 and Figures S11–12 in the SI for IR spectra and analytical HPL chromatograms).

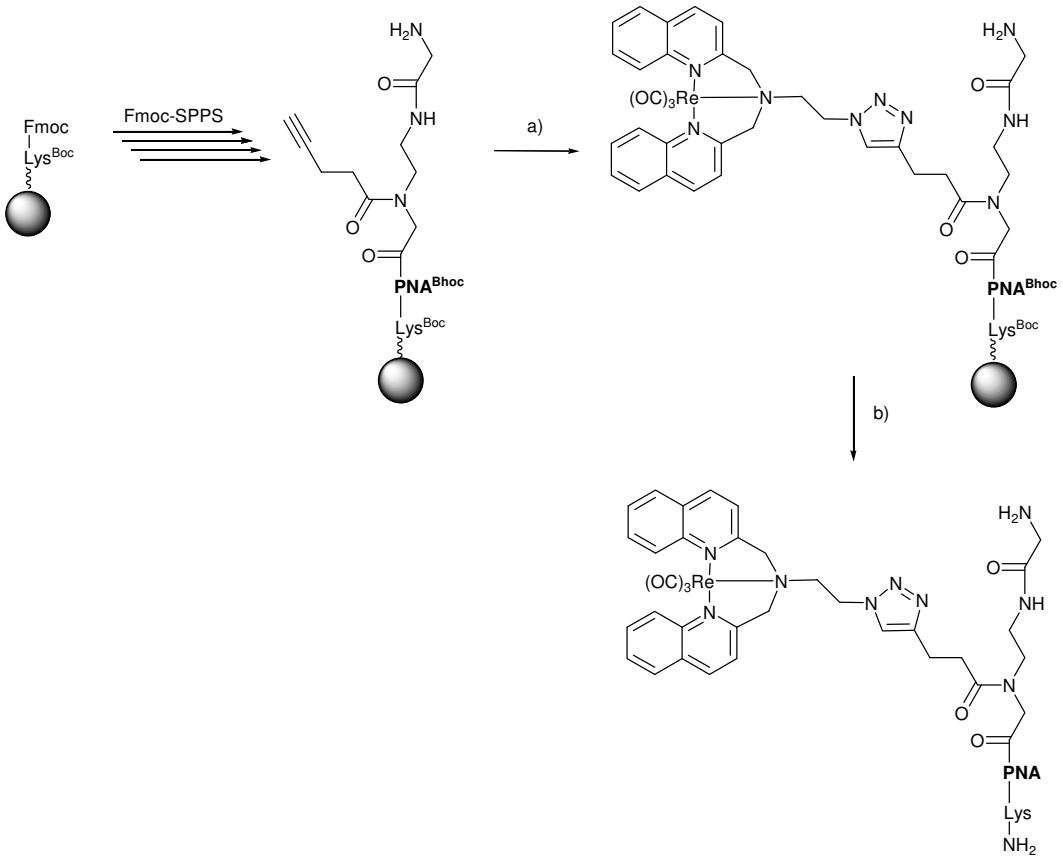

Scheme 2. Synthesis of Re-containing PNA oligomers. (a) i) CuI, **[Re(CO)$_3$(L-N$_3$)]Br**, DIPEA, DMF; ii) Washing with DMF, CH_2Cl_2 and DMF; (b) TFA:phenol:TIS 85:10:5 V/V/V.

Thermal stability studies. In order to determine the influence of the Re complex or the rhodamine fluorophore on the stability of DNA/RNA•PNA hybrids, we studied the thermal stability of our PNAs, namely **Re-PNA**, **Rho-PNA** and **Naked-PNA** with the 23-mer DNA sequence 5'-

GCAAGCTGACCCTGAAGTTCAT -3'. This DNA sequence was used as a model for the mRNA that we will target in future studies. All UV-Vis melting spectra of PNA-DNA can be seen in the SI (Figures S13-18). As shown in Table 3, we did not observe any differences between **Re-PNA** and **Rho-PNA** with melting temperatures (T_ms) of approximatively 85°C, whilst the T_m of **Naked-PNA** was slightly lower at approximatively 82°C. This indicates that both the Re complex and the rhodamine fluorophore actually stabilize the PNA•DNA hybrid, possibly through electrostatic interactions with the negatively charged DNA backbone. Any difference observed in the antisense effects between **Re-PNA** and **Rho-PNA** should hence be due to reasons other than PNA•DNA (and PNA•mRNA, respectively) hybrid stability.

Table 3. Melting temperatures (T_m / °C) of PNA•DNA hybrids (DNA sequence: 5'-GCAAGCTGACCCTGAAGTTCAT -3'.

PNAs	T_m / °C
Naked-PNA	82.2 ± 0.3
Rho-PNA	85.3 ± 0.1
Re-PNA	85.3 ± 0.1

Spectroscopic properties of Re-PNA and Re-PNA•DNA. The emission spectra for **Re-PNA** and its **Re-PNA•DNA** hybrid were recorded at 2 μM strand concentrations in PBS buffer (pH 7.4) after excitation at 347 nm. The hybrid formation was induced by heating the equimolar solutions at 90 °C for 15 min followed by slowly cooling to room temperature over a period of 2 h. To ensure duplex formation, a thermal program from 4°C to 90°C was repeated three times (see experimental section for more details). As shown in Figure 5 (dotted line), the emission spectrum for **Re-PNA** exhibited maxima at 397, 432 and 564 nm. Upon hybridisation with the complementary DNA strand (**DNA**), the

position of the maxima and emission intensity for the hybrid **Re-PNA•DNA** (Figure 5, solid line) remained mainly unchanged compared to those of the single strand **Re-PNA** – viz. the maxima of **Re-PNA•DNA** are located at 397, 433 and 574 nm, respectively. This suggests that the photophysical properties stay more or less unaffected by the hybridisation process.

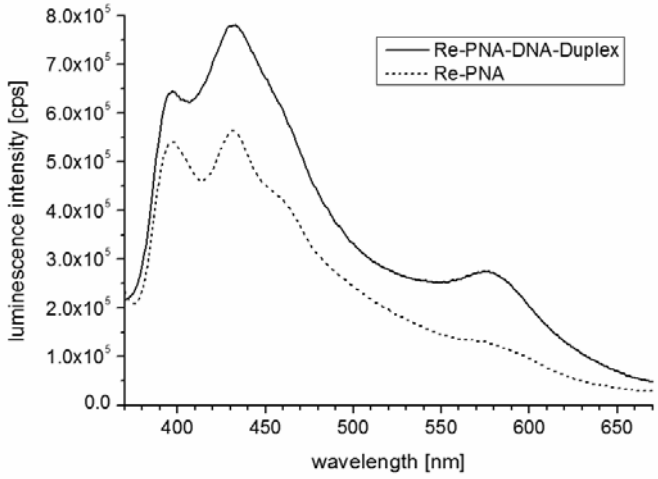

Figure 5. Comparison of the emission spectra of **Re-PNA** (dotted line) and its duplex with the complementary **DNA** (solid line) (2 μM in 0.1 M PBS (pH 7.4) buffer) (λ_{exc} = 347 nm).

***In vitro* fluorescence studies.** With the Re-containing sequence in hand and having established that **[Re(CO)$_3$(L-N$_3$)]Br** had the required properties for a fluorescent probe, we examined the possibility to use the Re complex to localize the PNA bioconjugates within a cell, as previously undertaken by Zubieta, Vaillant *et al.* with other Re-tricarbonyl bioconjugates[20, 21, 24, 25, 28] and very recently by Licandro *et al.* with a di-rhenium complex-containing (t)$_{10}$-PNA decamer.[12] HeLa cells were transfected with **Re-PNA** by electroporation and the presence of **Re-PNA** within the cell was unambiguously confirmed by fluorescent microscopy (Figure 6). A minimal concentration of 10 μM was necessary to allow detection of the Re bioconjugate. The detected fluorescence seemed to concentrate in the perinuclear region. Similarly, **Rho-PNA** was also transfected into HeLa cells and likewise, a concentration of 10 μM was required to allow good imaging of the cells (see Figure S19 in

the SI) suggesting that the Re complex is well-suited for cellular imaging when such concentrations are required. PNA are indeed used in the low micromolar range for cellular antisense purposes.[50] Of note, no intrinsic cytotoxic effects of the **Re-PNA** and **Rho-PNA** bioconjugates were visually observed at the concentrations up to 25 μM. The cells were viable after 48h. These results further support the use of organometallic-PNA bioconjugates for *in vitro* applications.

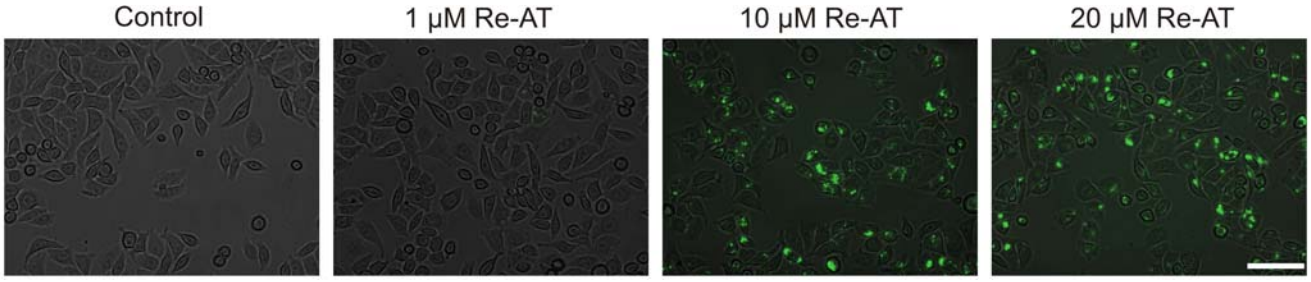

Figure 6. Fluorescence micrographs of HeLa cells 24 h after delivery of three different concentrations of **Re-PNA** by electroporation. Scale bar indicates 50 μm in all images.

Conclusion

In this study, the conjugation of a new fluorescent rhenium tricarbonyl complex, **[Re(CO)$_3$(L-N$_3$)]Br**, to a PNA oligomer was successfully carried out using the copper(I)-catalyzed Huisgen azide-alkyne cycloaddition reaction (Cu-ACC, "click" chemistry) to give **Re-PNA**. The coupling could be successfully performed on the solid phase, underscoring the good stability of the new Re complex. Full photophysical characterization confirms the assumed favourable properties of the Re complex, namely a large Stokes shift, good quantum yields and long fluorescence lifetime. Importantly, it was demonstrated that upon hybridisation with the complementary DNA strand (**DNA**), the position of the maxima and emission intensity for the hybrid **Re-PNA•DNA** remained mainly unchanged compared to those of the single strand **Re-PNA**. This suggests that the photophysical properties stay more or less unaffected by the hybridisation process. These favourable properties translate well into *in vitro* fluorescence microscopy. The new Re-containing PNA oligomer could be indeed detected in living cells using fluorescent microscopy at a concentration of 10 μM. These findings emphasize that organometallic-containing PNAs can indeed be employed for *in vitro* experiments, contrary to the general notion that organometallic compounds are usually unstable under physiological conditions and/or cytotoxic. In combination with previously reported techniques of quantitative uptake and localization studies of metal bioconjugates in general,[10-12] the results reported herein pave the way to further development metal-PNA conjugates for biomedical studies. Indeed, preliminary data suggest that the metal-PNA conjugates described herein may indeed be used as anti-sense agents. An 18 % decrease of expression of the eGFP protein could be observed in genetically modified HeLa cells 48 h after incubation with a metal-PNA conjugate targeting the eGFP sequence. Notably, no change in protein expression was observed with a conjugate containing a mismatched PNA sequence, suggesting a specific antisense effect. While these results are encouraging for the use of metal-PNA conjugates as promising multi-functional tools in cell biology, there is certainly scope for optimization and experiments along these lines are currently carried out in our laboratories.

Experimental Section

Materials. All reactions were carried out in ordinary glassware and solvents were used without further precautions except if indicated. Chemicals were purchased from commercials suppliers and used as received. Solvents were used as received or dried over 4 Å molecular sieves.

Caution! Although no problems were encountered in this work, azide complexes are potentially explosive. They should be prepared in small quantities and handled with care.

Instrumentation and methods. *^{1}H and ^{13}C NMR spectra* were recorded in deuterated solvents on a Bruker DRX 400 spectrometer at 30°C. The chemical shifts, δ, are reported in ppm (parts per million). The residual solvent peaks have been used as an internal reference. The abbreviations for the peak multiplicities are as follows: s (singlet), d (doublet), dd (doublet of doublets), t (triplet), q (quartet), m (multiplet) and br (broad). *Infrared spectra* were recorded on a ATR unit using a Bruker Tensor 27 FTIR spectrophotometer at 4 cm^{-1} resolution. Signal intensity is abbreviated br (broad). *ESI mass spectra* were recorded on a Bruker Esquire 6000. All UV-Vis measurements were carried out on a VARIAN Cary 100 Conc instrument using quartz cuvettes of 1 cm width. The *matrix-assisted laser desorption/ionization time of flight mass spectrometry (MALDI-ToF) mass spectra* were measured on a Bruker Daltonics Autoflex. The experiments were performed in linear mode with positive polarity using sinapinic acid as the matrix. *HPLC purification* was performed on an Agilent Series 1100 system equipped with a C18 Nucleodur gravity column (125 x 21 mm, 5 µm particle size, Macherey-Nagel). Preparative (flowrate: 10.0 mL min^{-1}) runs were performed with a linear gradient of A (millipore® water containing 0.1 % v/v TFA) and B (acetonitrile (Baker HPLC-grade), containing 0.1 % v/v TFA): t = 0 min 5 % B. t = 35 min 52 % B. t = 45 min 100 % B. t = 55 min 100 % B. t = 60 min 0 % B. LC-MS experiments were performed on an Agilent 1100 series HPLC system connected to a Thermo LCQ Advantage mass spectrometer equipped with an electrospray ion source. A C18 Nucleodur gravity column (125 x 4 mm, 3 µm particle size, Macherey-Nagel) was used for small molecules. Material was

eluted using a gradient system of acetonitrile (B) and water containing 0.1% formic acid (A) and a flow rate of 1 mL min^{-1}. t = 0-1 min (10 % B), t = 1-10 min (from 10 to 100 % B), t = 10-12 min (100 % B).

Synthesis and Characterization.

2-(bis((quinolin-2-yl)methyl)amino)ethanol (L-OH). L-OH was prepared following the procedure published by Zubieta *et al*.[31]

2-(*N*-(2-(((9*H*-fluoren-9-yl)methoxy)carbonylamino)ethyl)pent-4-ynamido)acetic acid (Fmoc-1-OH). Fmoc-1-OH was prepared following the procedure published by Gasser *et al*.[44] The spectroscopic data of the products matched that reported previously.[44]

$[NEt_4][ReBr_3(CO)_3]$. $[NEt_4][ReBr_3(CO)_3]$ was prepared following the procedure published by Alberto *et al*. The spectroscopic data of the products matched that reported previously.[33]

2-azido-*N*,*N*-bis((quinolin-2-yl)methyl)ethanamine (L-N_3). To a solution of 2-(bis((quinolin-2-yl)methyl)amino)ethanol (1.00 g, 2.91 mmol) and triphenylphosphine (1.54 g, 5.82 mmol) in dry THF (40 mL) was slowly added diisopropyl azodicarboxylate (1.218 mL, 5.82 mmol) under a nitrogen atmosphere. The mixture was stirred for 5 min before diphenylphosphoryl azide (1.294 mL, 5.82 mmol) was slowly added to the solution. The reaction mixture turned from brown to dark brown with the appearance of a white precipitate. The mixture was stirred for 72h at room temperature, time during the precipitate disappeared. The solvent of the reaction mixture was then evaporated to dryness to give a brown oil. In order to remove the major impurities of the product (excess reagents), this oil was dissolved in CH_2Cl_2 (100 mL) and the compound was transferred into the aqueous phase with 1M $HCl_{(aq)}$ (3x75 mL) (the majority of the reagents stay in the organic phase). The combined aqueous phases were rendered basic (pH = 13) with 5M $NaOH_{(aq)}$ and extracted with CH_2Cl_2 (3x100 mL). The combined organic phases were then concentrated under vacuo to give a brown oil. A purification by column chromatography on neutral alumina was then performed using CH_2Cl_2:MeOH 100:0.5 as the eluent to give a slightly yellow solid (Rf = 0.25). Yield. 0.34 g (32 %). **Characterization Data.** Analyses Found (%): C, 71.82; H, 5.00; N, 22.56. Calcd for $C_{14}H_{16}N_6$ (%): C, 71.72; H, 5.47; N, 22.81.

IR bands (ν, cm^{-1}): 3057 w, 2967 w, 2929 w, 2841 w, 2185 w, 2093 s, 1971w, 1715 w, 1666 w, 1600 m, 1563 w, 1500 m, 1451 w, 1424 m, 1361 w, 1295 br m, 1116 w, 1036 w, 1007 w, 965 m, 944 w, 882 w, 829 s, 796 m, 764 m, 644 w, 617 w. ^{1}H NMR Spectrum ($CDCl_3$): δ 2.92 (t, ^3J = 5.9 Hz, 2H, N-CH_2-CH_2), 3.34 (t, ^3J = 5.9 Hz, 2H, CH_2-CH_2N_3), 4.08 (s, 4H, N-CH_2-quin), 7.49 (m, 2H, C*H* quin), 7.64-7.80 (m, 6H, C*H* quin), 8.03 (m, 2H, C*H* quin), 8.14 (m, 2H, C*H* quin). ^{13}C NMR Spectrum ($CDCl_3$): δ 49.4 (CH_2-*C*H_2N_3), 54.0 (N-*C*H_2-CH_2), 61.9 (N-*C*H_2-pyr), 121.3 (*C*H), 126.5 (*C*H), 127.7 (*C*), 127.8 (*C*H), 129.3 (*C*H), 129.7 (*C*H), 136.7 (*C*H), 147.8 (*C*), 160.0 (*C*, all from the quinoline ligands). Electrospray Mass Spectrum (*m/z*): 369.1 $[M+H]^+$ (100%), 391.1 $[M+Na]^+$ (63%). High-Resolution Mass Spectrum (EI): calcd. for $C_{22}H_{20}N_6$ ($[M]^+$): 368.1749; found: 368.1749.

Rhenium tricarbonyl complex of L-N_3 ([Re(CO)$_3$(L-N_3)]Br). 2-azido-*N*,*N*-bis((quinolin-2-yl)methyl)ethanamine (50 mg, 0.14 mmol) and $[NEt_4]_2[ReBr_3(CO)_3]$ (105 mg, 0.14 mmol) were refluxed in deoxygenated methanol (20 mL) for 3h. The reaction mixture, which turned yellow-brown, was evaporated to dryness. A purification by column chromatography on silica with a gradient of CH_2Cl_2:MeOH 100:7 to CH_2Cl_2:MeOH 10:1 as the eluent (Rf = 0.38 in CH_2Cl_2:MeOH 10:1) was performed to give a slightly yellow solid. Crystals suitable for X-ray crystallography were grown by letting slowly evaporated a solution of **[Re(CO)$_3$(L-N_3)]Br** in CD_3OD over 3 days. Yield. 80 mg (84 %). **Characterization Data.** Major IR bands (ν, cm^{-1}): 3389 br w, 3057 w, 2925 w, 2101 m, 2025 s, 1897 s, 1715 w, 1601 w, 1568 w, 1514 w, 1464 w, 1434 w, 1370 w, 1343 w, 1290 w, 1259 w, 1209 w, 1145 w, 1125 w, 1086 w, 1028 w, 972 w, 916 w, 871 w, 825 w, 781 w, 749 w, 646 w.^{1}H NMR Spectrum (CD_3OD, just after dissolution): δ 4.13 (s, br, 4H, N-CH_2-CH_2 and CH_2-CH_2N_3), 5.21 (d, ^2J = 17.7 Hz, 2H, N-CH_2-quin), 5.30 (d, ^2J = 17.7 Hz, 2H, N-CH_2-quin), 7.69 (m, 4H, C*H* quin), 7.86 (m, 2H, C*H* quin), 8.01 (m, 2H, C*H* quin), 8.52 (m, 4H, C*H* quin). ^{13}C NMR Spectrum (CD_3OD, long after dissolution): δ 49.6 (CH_2-*C*H_2N_3) (under the MeOD peak), 67.1 (N-*C*H_2-CH_2), 68.0 (m, N-*C*H_2-pyr), 121.1 (*C*H quin), 129.6 (*C*H quin), 129.6 (*C*H quin), 130.0 (*C* quin), 131.0 (*C*H quin), 134.2 (*C*H quin), 143.1 (*C*H quin), 148.3 (*C* quin), 166.3 (*C* quin), 195.4, 197.1 (*fac*-Re(CO)$_3$). Electrospray Mass

Spectrum (*m/z*): 639.0 $[M]^+$ (100%). High-Resolution Mass Spectrum (EI): calcd. for $C_{25}H_{20}N_6O_3Re$ ($[M]^+$): 639.1154; found: 639.1192.

Peptide nucleic acid synthesis. The PNAs were prepared by solid-phase peptide synthesis (SPPS). SPPS was performed manually in 5 mL polypropylene one-way syringes as reaction vessels, which were equipped with a frit at the bottom. They were filled with 125 mg of polystyrene resin beads TentaGel R RAM Lys(Boc)Fmoc (0.18 mmol/g) from Rapp Polymere. The resin was swollen in DMF before use for 1 h. All reactions were performed on a mechanical shaker at 400 rpm, soaking approximately 3-4 mL of freshly prepared solutions into the syringe. Fmoc/Bhoc protected PNA monomers or the Fmoc-spacer (5 eq) (all from Link Technologies, Lanarkshire, Scotland) were preactivated in Eppendorf tubes before every coupling step for 2 min with HATU (4.5 eq) in DMF, adding DIPEA and 2,6-lutidine (10 eq each) (A(bhoc)-PNA-monomer: 5 min, C(bhoc)-PNA-monomer: 7 min). For each coupling step the resin beads were treated with the activated acid under vibration and subsequently washed with DMF. The coupling step was monitored with the Kaiser test. Double Fmoc deprotection was performed with piperidine (20 %, v/v) in DMF (2 min + 10 min). The resin beads were then washed successively with DMF, DCM and DMF. The whole procedure (deprotection, coupling, monitoring) was repeated for every PNA monomer until the PNA sequence was completed. The insertion of the synthon **Fmoc-1-OH** into the PNA oligomers was performed according to the general SPPS procedure. Before cleavage, the resin was shrunk with methanol and dried. The non-rhenium containing PNAs were then cleaved using a mixture of trifluoroacetic acid:water:triisopropylsilane 95:2.5:2.5 v/v/v while the rhenium containing PNAs were cleaved using a mixture of TFA:phenol:TIS 85:10:5 V/V/V [3 x 400 µl (1h30 each)]. The resulting solutions were first evaporated to dryness before being precipitated with ice-cold ether. The solids were centrifuged, washed with ice-cold ether and finally air dried. The obtained crude oligomers were lyophilized in acetonitrile / water, purified and analyzed with RP-HPLC and finally characterized with ESI or MALDI-TOF mass spectrometry.

General procedure for the synthesis of Rhodamine-containing PNA oligomers. These oligomers were prepared using a similar method to this one developed by Corey *et al*.[43] The PNA sequence to be labelled containing resin (2 μmol) was introduced into a fritted syringe and was subsequently swollen with DMF for 1h. Sulforhodamine (15.7 mg) dissolved in a mixture DIPEA:DMF 1:30 v/v (500 μL) was introduced into the syringe and the mixture was shaken for 30 min., at r.t., in the dark. The resin was then thoroughly washed with a mixture of DMF:CH_2Cl_2 v/v to remove unbound sulforhodamine. The *N*-terminal Fmoc protecting group of the PNA sequence was then removed using a mixture Piperidine 20% in DMF (2 x 10 min). The resin was again washed with DMF. 5-(and -6)-carboxytetramethylrhodamine succinimidyl ester (supplied as a mixture of isomers) (6 mg) dissolved in a mixture of DIPEA:DMF 1:30 v/v (500 μL) was introduced to the syringe and the mixture was shaken for 21h, at r.t., in the dark. The resin was then washed thoroughly with DMF. See above for the details of the subsequent cleavage of the resin.

General procedure for the synthesis of Rhenium-containing PNA oligomers by Click Chemistry. The synthon **1** containing PNA resin was shrunk with methanol, dried over vacuum and then transferred into a fritted syringe. The resin was then swollen with DMF for 1h. The *N*-terminal Fmoc protecting group of the PNA sequence was then removed using a mixture of piperidine 20% in DMF (2 x 10 min). The resin was again washed with DMF. **[Re(CO)$_3$(L-N$_3$)]Br** (3.0 eq.) and CuI (2.5 eq.) were then introduced into the syringe (from the top). Afterwards, a mixture of ethyldiisopropylamine (54 μL) and DMF (400 μL) were aspired up the syringe and the mixture was shaken for 3 days at room temperature in the absence of light and under an argon atmosphere. The resin was then washed with DMF (5x), CH_2Cl_2 (5x) and DMF (5x) successively. See above for the details of the subsequent cleavage of the resin.

Calculation of the Extinction Coefficient of Re(CO)$_3$(L-N$_3$)]Br. The extinction coefficient of the rhenium complex in the PNA oligomer was estimated using **Re(CO)$_3$(L-N$_3$)]Br** as model compound. The absorption of **Re(CO)$_3$(L-N$_3$)]Br** in H_2O at 80°C at 260 nm was measured in the concentration

range of 20 – 50 μM with increments of 10 μM. The gradient of the linear plot of the absorption against the concentration allows for the calculation of the extinction coefficient, $\varepsilon_{260} = 9040\ M^{-1}cm^{-1}$.

PNA Concentration Determination. PNA concentration was measured by means of the absorption at 260 nm using the incremental extinction coefficients of the PNA ($\varepsilon_{PNA,A} = 13700\ M^{-1}cm^{-1}$, $\varepsilon_{PNA,G} = 11700\ M^{-1}cm^{-1}$, $\varepsilon_{PNA,C} = 6600\ M^{-1}cm^{-1}$, $\varepsilon_{PNA,T} = 8600\ M^{-1}cm^{-1}$) for the Re-containing PNA oligomers[2] and at 555 nm for the rhodamine-containing PNA oligomers using 65000 cm^{-1} as the extinction coefficient. The different PNAs were dissolved in MQ water and then filtered to produce stock solutions. Small aliquots of these stock solutions were then highly diluted in Phosphate Buffer (100 mM, pH = 7.4). The measurements were carried out at 80°C where the PNA strands are completely destacked for the naked and Re-containing PNA oligomers and at 20°C for rhodamine-containing PNA oligomers.

Thermal stability studies. Solutions of PNA and DNA oligomers were all brought to 3 μM in phosphate buffer, pH = 7.4. The duplexes were annealed at 90°C for 15 min and then cooled down slowly to room temperature in the spectrometer. Thermal program: starting and returning temperature was 25°C. Heating to 90°C, cooling to 4°C, each at 0.5°C/min and holding for 3 min at the end-temperatures. The procedure was repeated three times.

Re-PNA and Re-PNA•DNA sample preparation for fluorescence measurements. Fluorescence measurements were performed with solutions of 2 μM **Re-PNA** and of 2 μM of the hybrid **Re-PNA•DNA**, each in 0.1 M PBS buffer, pH = 7.4. The preparation of the hybrid **Re-PNA•DNA** is similar to those of the thermal stability studies. Shortly, the hybrid formation was induced by heating the equimolar solutions of **Re-PNA** and **DNA** at 90 °C for 15 min and then cooled down slowly to room temperature in the spectrometer. To ensure duplex formation the thermal program was done subsequently: starting and returning temperature was 25°C. Heating to 90°C, cooling to 4°C, each at 0.5°C/min and holding for 3 min at the end-temperatures. The procedure was repeated three times.

Fluorescence measurements. Steady state emission spectra were acquired on a PTI Quantamaster QM4 spectrofluorimeter[51] using 1.0 cm quartz cuvettes. The excitation light source was a 75 W continuous xenon short arc lamp. Emission and excitation spectra were collected at 90° to the excitation beam using a PTI R928 photomultiplier tube (operated at -1000 V) as the detector. Spectral selection was achieved by single grating monochromators (1200 grooves/mm, blazed at 300 nm for the excitation and at 400 nm for the emission). Quantum yields were measured with optically dilute solutions ($A < 0.1$) using the following equation:

$$\frac{\Phi_x}{\Phi_r} = \left[\frac{A_r(\lambda_r)}{A_x(\lambda_x)}\right]\left[\frac{I(\lambda_r)}{I(\lambda_x)}\right]\left[\frac{\eta_x^2}{\eta_r^2}\right]\left[\frac{D_x}{D_r}\right]$$

where A is the absorbance at the excitation wavelength (λ), I is the intensity of the excitation light at the same wavelength, η is the refractive index and D is the integrated luminescence intensity of the respective emission peak. The integrals of the two emission peaks at ca. 430 nm and ca. 560 nm were deconvoluted by a fitting procedure with two overlapping Voigt functions using Origin Pro 8G.[52] The subscripts 'x' and 'r' refer to the sample and reference respectively. Quantum yields were determined relative to quinine sulfate hemihydrate (in 0.5 M sulfuric acid, $\Phi_r = 0.546$) as standard.[53] The estimated errors for the obtained values are ± 30%.

Luminescence lifetimes were measured with the same PTI Quantamaster QM4 spectrofluorimeter equipped with an additional Q4 phosphorescence module. The light source for these measurements was a xenon flash lamp (Hamamatsu L4633: 100 Hz repetition rate, pulse width ca. 1.5 μs FWHM). Emission was measured at 90° using a PTI P1.7R detector module (Hamamatsu PMT R5509-72 with a Hamamatsu C9525 power supply operated at -1500 V and a Hamamatsu liquid N_2 cooling unit C9940 operated at -80°C). Spectral selection of the emission was achieved by passage through a single grating emission monochromator (1200 grooves/mm, blazed at 400 nm). The instrument response function was determined using a dilute aqueous solution of colloidal silica (Ludox® AM-30). Lifetime data analysis

(deconvolution, statistical parameters, etc.) was performed using the software package FeliX32 from PTI.[51] The given values are averages of three independent measurements. Estimated error values for the obtained lifetimes are ± 20%.

Cell Culture. Experiments were performed on human cervix epithelial cells (HeLa). The cells were cultured in CCM (cell culture medium: Dulbecco's modified Eagle's medium (DMEM) supplemented with 10% fetal calf serum (FCS), 2 mM glutamine, 100 U mL^{-1} penicillin, 100 µg mL^{-1} streptomycin) in T 75 flasks (Sarstedt, Nümbrecht, Germany) at 37°C and 10% CO_2. All media and reagents were purchased from PAA, Cölbe, Germany. The cells were split by tripsination (2.5 mg/ml Trypsin with 0.02M EDTA) and subcultivated every 4-7 days.

Cell Transfection – Electroporation (fluorescent microscope measurements). PNA was delivered by electroporation using the Amaxa Cell Line Nucleofactor® Kit R (Lonza Cologne AG, Köln, Germany) according to the manufactures' manual. In short after cell harvesting a cell pellet of 1 x 10^6 cells was resuspended in 100 µL Nucleofector® Solution and supplemented with 1, 10 or 20 µM of PNA. Nucleofection® was carried out using the Nucleofector® Program I-13. Afterwards the cells were transferred into an excess of pre-equilibrated CCM and shortly centrifuged at 80xg. Finally 5 x 10^5 cells per well were cultivated in 24 well plates (TPP, Trasadingen, Switzerland) at 37°C and 10% CO_2. As a control, cells were electroporated without delivering any target.

***In vitro* Fluorescence Evaluation.** The cellular localization of the fluorescent PNA bioconjugates was confirmed by fluorescence microscopy. Different concentrations (1, 10 and 20 µM) of **Re-PNA** or **Rho-PNA** respectively were electroporated into HeLa cells as described above. One day after delivery the CCM was removed by phosphate buffered saline (PBS) and microscopic pictures were taken from live cells. The Re bioconjugate was excited between 330 - 385 nm and the fluorescence was detected at >420 nm on an Olympus IX 81 motorized inverted microscope (Olympus, Hamburg, Germany). The Rho complex was excited by a HeNe laser at 543 nm and the fluorescence was detected in the range of 548 nm to 698 nm on a Zeiss Axioplan LSM 510 meta microscope.

X-ray Crystallography. Crystallographic data for **Re(CO)$_3$(L-N$_3$)]Br** have been deposited with the Cambridge Crystallographic Data Centre as supplementary publication (CCDC no. 757065). Copy of the data can be obtained, free of charge, on application to CCDC, 12 Union Road, Cambridge CB2 1EZ, UK, (fax: +44-(0)1223-336033 or e-mail: deposit@ccdc.cam.ac.uk or via www.ccdc.cam.ac.uk/data_request/cif). Crystallographic data for **Re(CO)$_3$(L-N$_3$)]Br**. $C_{52}H_{46}Br_2N_{12}O_8Re_2$, M = 1499.23, triclinic, space group *P-1*, a = 9.707(5), b = 10.899(5), c = 12.796(6) Å, α = 74.586(9), β = 85.97(1), γ = 86.817(9)^o, V = 1300.9(11) Å^3, Z = 1, $2\theta_{max}$ = 50.23^o, 7168 measured reflections, 4498 independent reflections, 338 parameters, μ = 6.251 mm $^{-1}$, $R1$ = 0.0632 for 4358 observed reflections ($I > 2\sigma(I)$), $wR2$ = 0.1641for all reflections. Bruker-axs-SMART 1000 CCD. Structure solution with direct methods (SHELXS97), and refined against F^2 with all measured reflections (SHELXL97[18] Platon/Squeeze[19]).

Acknowledgments. This work was supported by the Swiss National Science Foundation (Ambizione Fellowship N° PZ00P2_126404 and Professorship N° PP00P2_133568 to G.G.), the Alexander von Humboldt Foundation (fellowship to G.G.), the Research Department Interfacial Systems Chemistry and the DFG through the Research Unit "Biological Function of Organometallic Compounds" (FOR 630, www.rub.de/for630). G.G is grateful to Dr. Jacqui F. Young for her kind help for the purification of the PNA oligomers and MALDI-TOF measurements as well as to Prof. Dr. Roger Alberto for generous access to all the facilities of the Institute of Inorganic Chemistry of the University of Zurich. M.S. thanks the Fonds der Chemischen Industrie (Liebig fellowship) and the German Research Foundation (Emmy Noether fellowship) for financial support. We thank Prof. Dr. Dr. Dr. Hatt for generous access to his microscope and Dr. Christian Wetzel (Ruhr University Bochum, Faculty of Biology and Biotechnology, Department of Cell Physiology) for assistance in the microscopy experiment.

Supporting Information Available: NMR spectra of **L-N_3** and **[$Re(CO)_3$(L-N_3)]Br** (Figures S1-3), ESI-MS spectra of **[$Re(CO)_3$(L-N_3)]Br** (Figures S4-5), normalized absorption spectra of **$Re(CO)_3$(L-N_3)]Br** (Figure S6)**,** observed luminescence decay curves of **$Re(CO)_3$(L-N_3)]Br** (Figure S7), HPL chromatograms of **Naked-PNA** and **Rho-PNA** (Figure S8-9), MALDI-TOF mass spectra of **Rho-PNA** (Figure S10), HPL chromatograms of **Re-PNA** (Figure S11), ESI-MS characterisation of the **Re-PNA** (Table S1), IR Spectrum of **Re-PNA** (Figure S12), UV-Vis melting spectra of PNA-DNA (Figures S13-18), Fluorescent microscopy images of **Re-PNA** in HeLa cells (Figure S21). Crystallographic data for **$Re(CO)_3$(L-N_3)]Br** have been deposited with the Cambridge Crystallographic Data Centre as supplementary publication (CCDC no. 757065). Copy of the data can be obtained, free of charge, on application to CCDC, 12 Union Road, Cambridge CB2 1EZ, UK, (fax: +44-(0)1223-336033 or e-mail: deposit@ccdc.cam.ac.uk or via www.ccdc.cam.ac.uk/data_request/cif).

References

1. P. E. Nielsen, M. Egholm, R. H. Berg and O. Buchardt, *Science*, 1991, **254**, 1497.
2. P. E. Nielsen and M. Egholm, eds., *Peptide Nucleic Acids, Protocols and Applications*, Horizon Scientific Press, Wymondham, UK, 1999.
3. P. E. Nielsen, *Curr. Opin. Struct. Biol.*, 1999, **9**, 353.
4. U. Koppelhus and P. E. Nielsen, in *Antisense Drug Technology*, ed. S. T. Crooke, Marcel Dekker, New York, Editon edn., 2001, pp. 359.
5. J. C. Hanvey and L. E. Babiss, in *Delivery Strategies for Antisense Oligonucleotide Therapeutics* ed. S. Akhtar, CRC Press Inc., Boca Raton, Editon edn., 1995, pp. 151.
6. R. Gambari, *Curr. Top. Pharmacol.*, 2004, **8**, 313.
7. S. Cogoi, A. Codognotto, V. Rapozzi and L. E. Xodo, *Nucleos. Nucleot. & Nucleic Acids*, 2005, **24**, 971.
8. V. L. Marin, S. Roy and B. A. Armitage, *Expert Opin. Biol. Ther.*, 2004, **4**, 337.
9. G. Gasser, A. M. Sosniak and N. Metzler-Nolte, *Dalton Trans.*, 2011, **40**, 7061.
10. S. I. Kirin, I. Ott, R. Gust, W. Mier, T. Weyhermueller and N. Metzler-Nolte, *Angew. Chem., Int. Ed.*, 2008, **47**, 955.
11. A. Füssl, A. Schleifenbaum, M. Göritz, A. Riddell, C. Schultz and R. Kraemer, *J. Am. Chem. Soc.*, 2006, **128**, 5986.
12. E. Ferri, D. Donghi, M. Panigati, G. Prencipe, L. D'Alfonso, I. Zanoni, C. Baldoli, S. Maiorana, G. D'Alfonso and E. Licandro, *Chem. Comm.*, 2010, **46**, 6255.
13. C. A. Puckett and J. K. Barton, *J. Am. Chem. Soc.*, 2007, **129**, 46.
14. C. A. Puckett and J. K. Barton, *Biochemistry*, 2008, **47**, 11711.
15. C. A. Puckett and J. K. Barton, *J. Am. Chem. Soc.*, 2009, **131**, 8738.
16. C. A. Puckett and J. K. Barton, *Bioorg. Med. Chem.*, 2010, **18**, 3564.
17. C. A. Puckett, R. J. Ernst and J. K. Barton, *Dalton Trans.*, 2010, **39**, 1159.
18. S. James, K. P. Maresca, J. W. Babich, J. F. Valliant, L. C. Doering and J. Zubieta, *Bioconjugate Chem.*, 2006, **17**, 590.
19. L. Wei, J. W. Babich, W. C. Eckelman and J. Zubieta, *Inorg. Chem.*, 2005, **44**, 2198.
20. K. A. Stephenson, S. R. Banerjee, T. Besanger, O. O. Sogebin, M. K. Levadala, N. McFarlane, J. A. Lemon, D. R. Boreham, K. P. Maresca, J. D. Brennan, J. W. Babich, J. Zubieta and J. F. Valliant, *J. Am. Chem. Soc.*, 2004, **126**, 8598.
21. P. Schaffer, J. A. Gleave, J. A. Lemon, L. C. Reid, L. K. K. Pacey, T. H. Farncombe, D. R. Boreham, J. Zubieta, J. W. Babich, L. C. Doering and J. F. Valliant, *Nucl. Med. Biol.*, 2008, **35**, 159.
22. S. R. Banerjee, J. W. Babich and J. Zubieta, *Chem. Comm.*, 2005, 1784.
23. K. A. Stephenson, L. C. Reid, J. Zubieta, J. W. Babich, M.-P. Kung, H. F. Kung and J. F. Valliant, *Bioconjugate Chem.*, 2008, **19**, 1087.
24. S. James, K. P. Maresca, D. G. Allis, J. F. Valliant, W. Eckelman, J. W. Babich and J. Zubieta, *Bioconjugate Chem.*, 2006, **17**, 579.
25. N. Viola-Villegas, A. E. Rabideau, J. Cesnavicious, J. Zubieta and R. P. Doyle, *ChemMedChem*, 2008, **3**, 1387.
26. A. F. Armstrong, N. Oakley, S. Parker, P. W. Causey, J. Lemon, A. Capretta, C. Zimmerman, J. Joyal, F. Appoh, J. Zubieta, J. W. Babich, G. Singh and J. F. Valliant, *Chem. Comm.*, 2008, **43**, 5532.
27. A. F. Armstrong, J. Lemon, A., S. K. Czorny, G. Singh and J. F. Valliant, *Nucl. Med. Biol.*, 2009, **36**, 907.
28. N. Viola-Villegas, A. E. Rabideau, M. Bartholom, J. Zubieta and R. P. Doyle, *J. Med. Chem.*, 2009, **52**, 5253.

29. G. Gasser, S. Neumann, I. Ott, M. Seitz, R. Heumann and N. Metzler-Nolte, *Eur. J. Inorg. Chem.*, 2011, accepted.
30. L. Raszeja, A. Maghnouj, S. Hahn and N. Metzler-Nolte, *ChemBioChem*, 2011, **12**, 371.
31. M. K. Levadala, S. R. Banerjee, K. P. Maresca, J. W. Babich and J. Zubieta, *Synthesis*, 2004, **11**, 1759.
32. G. Gasser, K. Jäger, M. Zenker, R. Bergmann, J. Steinbach, H. Stephan and N. Metzler-Nolte, *J. Inorg. Biochem.*, 2010, **104**, 1133.
33. R. Alberto, A. Egli, U. Abram, K. Hegetschweiler, V. Gramlich and P. A. Schubiger, *J. Chem. Soc. Dalton Trans.*, 1994, 2815.
34. S. R. Banerjee, J. W. Babich and J. Zubieta, *Inorg. Chem. Commun.*, 2004, **7**, 481.
35. L. Wei, S. R. Banerjee, M. K. Levadala, J. Babich and J. Zubieta, *Inorg. Chem. Commun.*, 2003, **6**, 1099.
36. H. Yang, R. G. Carter and L. N. Zakharov, *J. Am. Chem. Soc.*, 2008, **130**, 9238.
37. J.-P. Zhang, Y.-Y. Lin, X.-C. Huang and X.-M. Chen, *J. Am. Chem. Soc.*, 2005, **127**, 5495.
38. A. J. Lees, *Chem. Rev.*, 1987, **87**, 711.
39. K. K.-W. Lo, K. H.-K. Tsang, W.-K. Hui and N. Zhu, *Chem. Comm.*, 2003, 2704.
40. N. Hüsken, G. Gasser, S. D. Köster and N. Metzler-Nolte, *Bioconjugate Chem.*, 2009, **20**, 1578.
41. T. Kersebohm, S. I. Kirin and N. Metzler-Nolte, *Bioorg. Med. Chem. Lett.*, 2006, **16**, 2964.
42. L. Christensen, R. Fitzpatrick, B. Gildea, K. H. Petersen, H. F. Hansen, T. Koch, M. Egholm, O. Buchardt, P. E. Nielsen, J. Coull and R. H. Berg, *J. Pept. Sci.*, 1995, **3**, 175.
43. L. D. Mayfield and D. R. Corey, *Biorg. Med. Chem. Lett.*, 1999, **9**, 1419.
44. G. Gasser, N. Hüsken, S. D. Köster and N. Metzler-Nolte, *Chem. Comm.*, 2008, 3675.
45. S. D. Köster, J. Dittrich, G. Gasser, N. Hüsken, I. Hernandez, J. L. Jios and N. Metzler-Nolte, *Organometallics*, 2008, **27**, 6326.
46. A. Sosniak, G. Gasser and N. Metzler-Nolte, *Org. Biomol. Chem.*, 2009, **7**, 4992
47. M. Patra, G. Gasser, D. Bobukhov, K. Merz, A. V. Shtemenko and N. Metzler-Nolte, *Dalton Trans.*, 2010, **39**, 5617.
48. G. Gasser, A. M. Sosniak, A. Leonidova, H. Braband and N. Metzler-Nolte, *Aust. J. Chem.*, 2011, **64**, 265.
49. G. Gasser, O. Brosch, A. Ewers, T. Weyhermüller and N. Metzler-Nolte, *Dalton Trans.*, 2009, 4310.
50. U. Koppelhus, T. Shiraishi, V. Zachar, S. Pankratova and P. E. Nielsen, *Bioconjugate Chem.*, 2008, **19**, 1526.
51. Photon Technology International Inc., Birmingham, NJ, USA, Editon edn.
52. Origin: OriginPro 8 SR1 (version 8.0773); OriginLab Corporation, Northampton, MA, USA, Editon edn., 2009.
53. W. H. Melhuish, *J. Phys. Chem.*, 1961, **65**, 229.